Supporting Information

Key role of persistent free radicals in soil for persulfate activation: Impacts to benzo[a]pyrene degradation

Yiwen Ou, [a] Xintong Li, [a] Shixu Feng [a] and Hongxia Zhao [a, *]

[a] Key Laboratory of Industrial Ecology and Environmental Engineering (Ministry of Education), School of Environmental Science and Technology, Dalian University of Technology, Dalian, 116024, China

[*]Corresponding author phone: +86-411-84706552; Fax: +86-411-84706552

Email: hxzhao@dlut.edu.cn

Text S1: Characteristics of soil sample

The amount of soil organic matter (SOM) was determined at 550 ℃, 4 h in a Muffle furnace. Soil pH was measured in 1:2.5 soil/water suspensions. X-ray Fluorescence Spectrometer (XRF, Axios, Panaco, Holland) was performed for understanding the inorganic element composition of the soil.

Text S2: ROS detection

As for the detection of ROS in the reaction system, persulfate solution was added to B[a]P contaminated soil and the spin trap DMPO and TEMP was 100 mM, respectively. Methanol salt solution was added as a •OH quencher for the detection of $•O_2^-$. A 10 μL suspension was collected by capillary tubes at different points in time to measure the ROS signal by EPR. Typical EPR instrument parameters were: center field at 3510 G, X-band microwave frequency of 9.85 GHz, microwave power of 1.70 mW, spectral window of 100 G, modulation amplitude of 1.00 G, modulation frequency of 100 kHz, time constant of 163.84 ms, conversion time 40.00 ms, sweep time 40.96 s and 5 times of X-scans.

Text S3: Extraction and fractionation of soil samples

After freeze-drying for 48 h, the soil samples were extracted and fractionated. The extraction details are as follows:[1] the freeze-dried soil samples were extracted treated by a mixing solution (ACE and DCM, 1:1, v/v) for 30 min in an ultrasonic environment. The supernatant was extracted by centrifugation at 3000 r/min for 10 min, repeated extraction for 3 times, then collected and combined the extraction. The total collected extracts were concentrated to 1 mL under a gentle nitrogen atmosphere. Subsequently, the concentrated extracts were cleaned up by the silica gel column, which contain 1 cm anhydrous sodium sulfate, 3 cm deactivated silica gel, 2 cm deactivated aluminium oxide and 2 cm anhydrous sodium sulfate from top to bottom. The silica gel column was activated with 10 mL HEX and eluted with 30 mL of HEX: DCM (7:3, v/v). The eluent containing B[a]P were collected, and then concentrated to near dryness with a nitrogen stream and reconstituted with ACN/HEX to a final volume of 1 mL transferring to a chromatographic vial. Before analysis, the extract was passed through a 0.22 m PTFE membrane.

Table S1. General assignments of FT-IR spectra of soil.

Wavenumber (cm^{-1})	**Mineral horizons**	**Organic horizons**	**Reference**
~3620	Clay O-H stretching	n/a	2
~3431	Water, stretching	O-H stretching (carboxylic acids/phenols/ alcohols); N-H stretching (amine/amide)	3
~2931, ~2848	n/a	C–H stretching (Aliphatics)	4
~1882	n/a	C=O stretching	5
~1639	n/a	C=C (aromatic structure); C=O (amides/quinones /COO^- /H-bonded conjugated ketones)	6
~1419	Mg–OH stretching	C–O stretching	7
~1014	Si–O stretching lattice	C-O stretching (polysaccharides/cellulose)	8
~908	Al-OH stretching OH bending modes of the inner hydroxyl groups of clay minerals	n/a	9
~773	Mg–OH, Al–OH	n/a	5
~690	SiO_2, Si–O–Si bending, lattice	n/a	5
~536, ~460	-Si-O bond	n/a	10

Table S2. B[a]P degradation intermediates were identified by GC-MS.

Peak	RT (min)	MW	formula	Product
P1	22.82	362	$C_{22}H_{34}O_4$	1,2-Benzenedicarboxylic acid, diheptyl ester
P2	19.37	282	$C_{20}H_{42}$	Eicosane
P3	17.81	278	$C_{16}H_{22}O_4$	Dibutyl phthalate
P4	16.43	270	$C_{17}H_{34}O_2$	Isopropyl myristate
P5	15.13	226	$C_{16}H_{34}$	Hexadecane
P6	12.85	206	$C_{14}H_{22}O$	2,4-Di-tert-butylphenol
P7	8.52	170	$C_{12}H_{26}$	Dodecane

Table S3. Toxicity classification according to the Globally Harmonized System of Classification and Labelling of Chemicals.

Level	Acute toxicity	Chronic toxicity
Not Harmful	$LC_{50}/EC_{50} > 100$ mg/L	ChV > 100 mg/L
Harmful	$10 < LC_{50}/EC_{50} \leq 100$ mg/L	$10 <$ ChV ≤ 100 mg/L
Toxic	$1 < LC_{50}/EC_{50} \leq 10$ mg/L	$1 <$ ChV ≤ 10 mg/L
Very Toxic	$LC_{50}/EC_{50} \leq 1$ mg/L	ChV ≤ 1 mg/L

Table S4. Estimated toxicity of B[a]P and degradation products.

Products	Acute toxicity (mg/L)			Chronic toxicity (mg/L)		
	Fish (96 h-LC_{50})	**Daphnid (48 h-LC_{50})**	**Green Alage (96 h-EC_{50})**	**Fish (ChV)**	**Daphnid (ChV)**	**Green Alage (ChV)**
B[a]P	0.042	0.035	0.125	0.0065	0.0098	0.076
P1	0.019	0.029	0.0053	0.0024	0.0012	0.0015
P2	0.000011	0.000013	0.00022	0.0000026	0.000010	0.00031
P3	0.893	0.748	0.527	0.079	0.143	0.205
P4	0.005	0.04	0.0074	0.00086	0.0017	0.0019
P5	0.0005	0.00051	0.004	0.000097	0.00024	0.0038
P6	0.144	0.133	0.206	0.02	0.031	0.067
P7	0.022	0.018	0.069	0.0034	0.0054	0.043

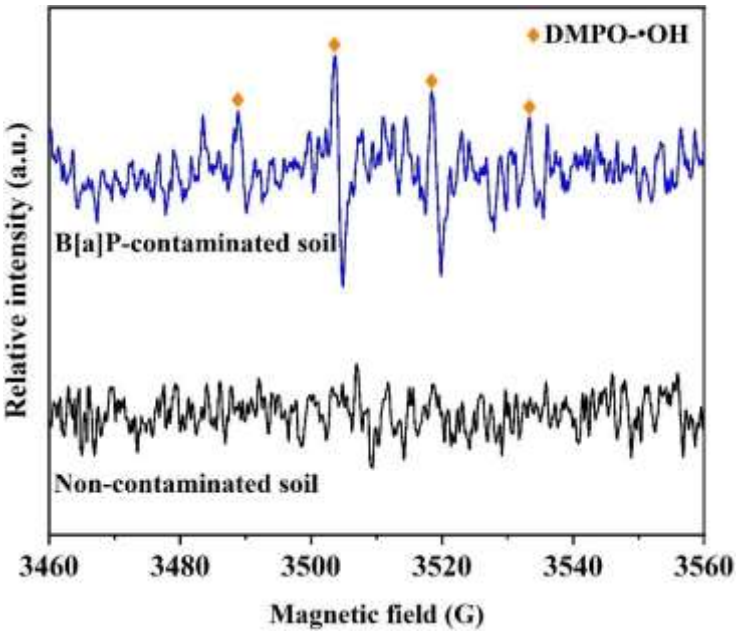

Fig. S1. DMPO-•OH in H_2O/B[a]P contaminated soil system.

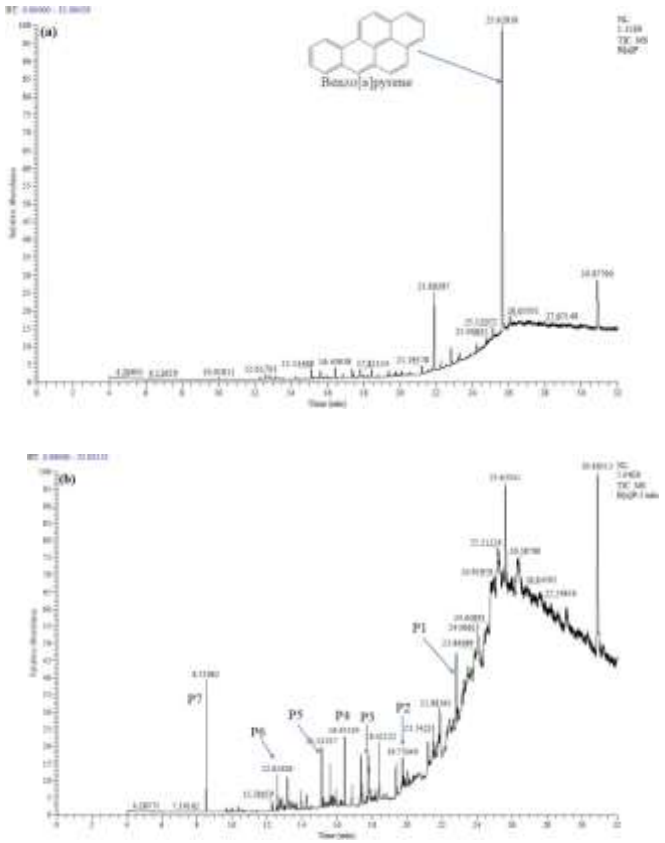

Fig. S2. GC-MS chromatogram of B[a]P- contaminated soil (a) and B[a]P transformation in persulfate system (b).

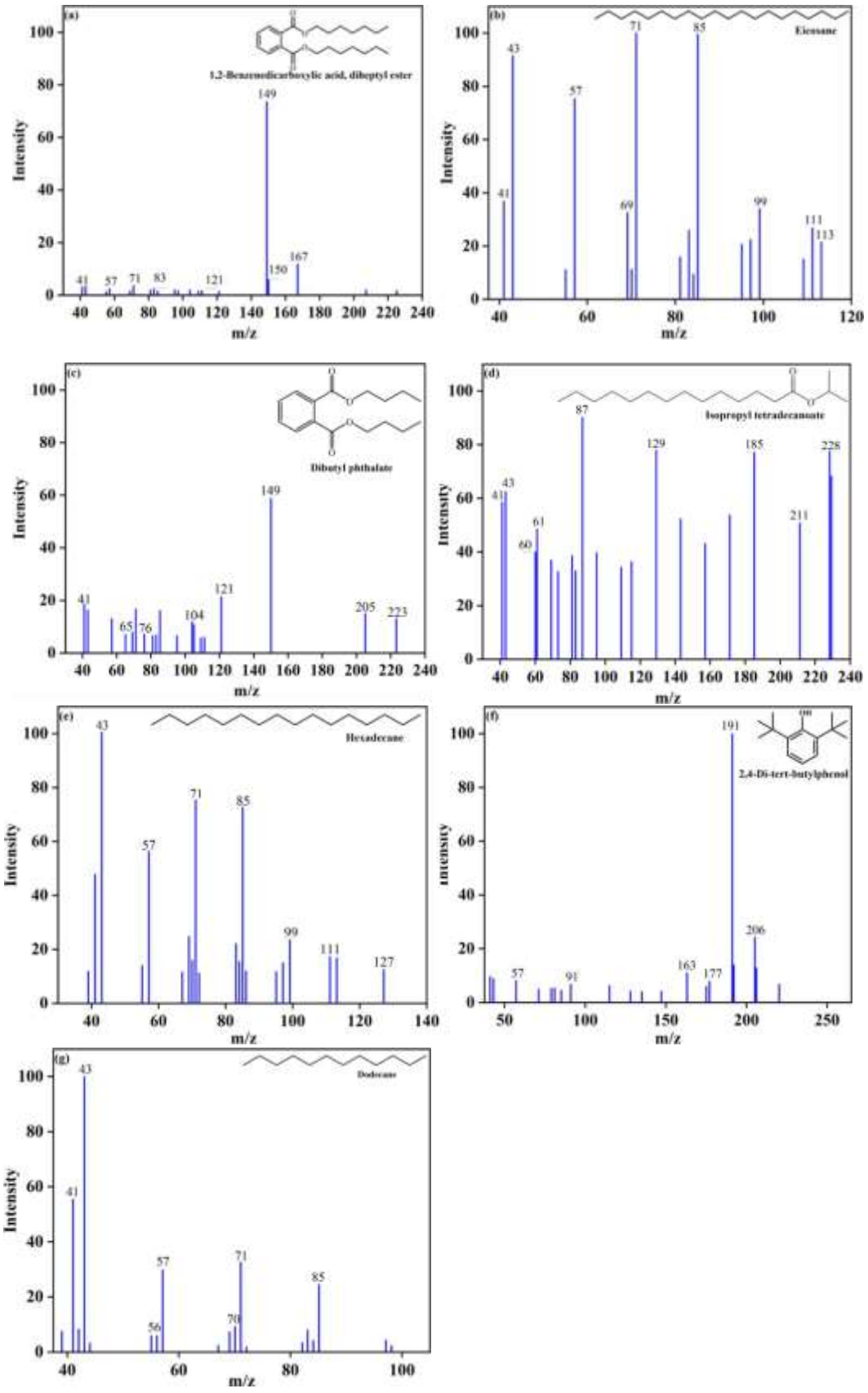

Fig. S3. The mass spectra of the derivatives of the possible intermediates.

References

1 X. N. Zhang, C. Y. Huang, J. Ren, T. G. Bekele and H. X. Zhao, Effect of cyclodextrin on desorption of petroleum hydrocarbons in soil, Process Safety and Environmental Protection, 2022, **160**, 199-208. http://doi.org/10.1016/j.psep.2022.02.023

2 F. Tivet, J. C. de Moraes Sá, R. Lal, D. M. B. P. Milori, C. Briedis, P. Letourmy, L. A. Pinheiro, P. R. Borszowskei and D. da Cruz Hartman, Assessing humification and organic C compounds by laser-induced fluorescence and FTIR spectroscopies under conventional and no-till management in Brazilian Oxisols, Geoderma, 2013, **207-208**, 71-81. http://doi.org/10.1016/j.geoderma.2013.05.001

3 C. Peltre, S. Bruun, C. Du, I. K. Thomsen and L. S. Jensen, Assessing soil constituents and labile soil organic carbon by mid-infrared photoacoustic spectroscopy, Soil Biology and Biochemistry, 2014, **77**, 41-50. http://doi.org/10.1016/j.soilbio.2014.06.022

4 R. Matamala, F. J. Calderón, J. D. Jastrow, Z. Fan, S. M. Hofmann, G. J. Michaelson, U. Mishra and C.-L. Ping, Influence of site and soil properties on the DRIFT spectra of northern cold-region soils, Geoderma, 2017, **305**, 80-91. http://doi.org/10.1016/j.geoderma.2017.05.014

5 P. K. Krivoshein, D. S. Volkov, O. B. Rogova and M. A. Proskurnin, FTIR photoacoustic spectroscopy for identification and assessment of soil components: Chernozems and their size fractions, Photoacoustics, 2020, **18**, 100162. http://doi.org/10.1016/j.pacs.2020.100162

6 C. Cocozzaa, V. D'Orazioa, T. M. Mianoa and W. Shotykb, Characterization of solid and aqueous phases of a peat bog profile using molecular fluorescence spectroscopy, ESR and FT-IR, and comparison with physical properties, Organic Geochemistry 2003, **34** 49–60 http://doi.org/doi.org/10.1016/S0146-6380(02)00208-5

7 A. M. Hofmeister and J. E. Bowey, Quantitative Infrared Spectra of Hydrosilicates and Related Minerals, Monthly Notices of the Royal Astronomical Society, 2006, **367**(2), 577-591. http://doi.org/10.1111/j.1365-2966.2006.09894.x

8 Z. Xing, K. Tian, C. W. Du, C. Y. Li, J. M. Zhou and Z. K. Chen, Agricultural soil characterization by FTIR spectroscopy at micrometer scales: Depth profiling by photoacoustic spectroscopy, Geoderma, 2019, **335**, 94-103. http://doi.org/10.1016/j.geoderma.2018.08.003

9 X. B. Xu, C. W. Du, F. Ma, Y. Z. Shen and J. Zhou, Forensic soil analysis using laser-induced breakdown spectroscopy (LIBS) and Fourier transform infrared total attenuated reflectance spectroscopy (FTIR-ATR): Principles and case studies, Forensic. Sci. Int., 2020, **310**, 110222. http://doi.org/10.1016/j.forsciint.2020.110222

10 Y. K. Li, Q. F. Liu, L. S. Liu, L. H. Liu, D. S. Hou and Y. K. Wu, Effect of original crystal size of kaolinite on the formation of intercalation compounds of coal-measure kaolinite, Materials Today Communications, 2023, **35**. http://doi.org/10.1016/j.mtcomm.2023.106130